Journal of Nuclear Medicine, published on July 2, 2021 as doi:10.2967/jnumed.121.262327

^{68}Ga-NODAGA-exendin-4 PET improves the detection of focal congenital hyperinsulinism

Marti Boss[1#], Christof Rottenburger[2*,3#], Winfried Brenner[4], Oliver Blankenstein[5], Vikas Prasad[4,6], Sonal Prasad[4,7], Paolo de Coppi[8], Peter Kühnen[5], Mijke Buitinga[1], Pirjo Nuutila[9,10], Timo Otonkoski[11,12], Khalid Hussain[13], Maarten Brom[1], Annemarie Eek[1], Jamshed Bomanji[3], Pratik Shah[14,15*], Martin Gotthardt[1]

[1] Department of Medical Imaging, Radboud University Medical Centre, Nijmegen, The Netherlands
[2]Division of Nuclear Medicine, University Hospital Basel, Switzerland
[3]Institute of Nuclear Medicine, University College London, UK
[4]Department of Nuclear Medicine, Charité - Universitätsmedizin Berlin, Germany
5 Institute for Experimental Pediatric endocrinology, Charité - Universitätsmedizin Berlin, Germany
[6]Department of Nuclear Medicine, University Hospital of Ulm, Germany
[7]Berlin Experimental Radionuclide Imaging Center (BERIC), Charité-Universitätsmedizin Berlin, Germany
[8]Department of Pediatric Surgery, Great Ormond Street Hospital for Children NHS Foundation Trust, London, UK
[9]Department of Endocrinology, Turku University Hospital, Turku, Finland
[10]Turku PET Center, University of Turku, Finland
[11]Stem cells and Metabolism Research Program, Faculty of Medicine, University of Helsinki, Finland
[12]Children's Hospital, University of Helsinki and Helsinki University Hospital, Finland
[13] Department of Pediatric Medicine, Division of Endocrinology, Sidra Medical and Research Center, Doha, Qatar
[14]Pediatric Endocrinology Department, Great Ormond Street Hospital for Children NHS Foundation Trust, London, UK
[15]Department of Pediatric Endocrinology, The Royal London Children's Hospital, Bart's Health NHS Trust, London , UK

**Current affiliation*
#Contributed equally to this work

Corresponding author
Marti Boss Msc, Postdoc
Geert Grooteplein-Zuid 10, 9101 HB, Nijmegen
Marti.boss@radboudumc.nl
+3124-3613813
Contact Marti Boss for reprint requests

Word Count: 4993

Running title: Exendin PET detects focal CHI

Financial disclosure

This work was supported by BetaCure (FP7/2014-2018, grant agreement 602812). PET/MR use at Charité was supported by Deutsche Forschungsgemeinschaft (INST 335/543-1 FUGG).

Disclaimer

M Gotthardt declares that he is an inventor and holder of the patent “Invention affecting GLP-1 and exendin” (Philipps-Universität Marburg, June 17, 2009). All other authors declare they no competing interests.

ABSTRACT

Surgery with curative intent can be offered to Congenital Hyperinsulinism (CHI) patients, provided that the lesion is focal. Radiolabeled Exendin-4 specifically binds the glucagon-like peptide 1 receptor (GLP-1R) on pancreatic beta cells. In this study we compared the performance of ^{18}F-DOPA positron emission tomography/computed tomography (DOPA PET), the current standard imaging method for CHI, and PET/CT with the new tracer ^{68}Ga-NODAGA-exendin-4 (Exendin PET) in the preoperative detection of focal CHI.

Methods

Nineteen CHI patients underwent both DOPA PET and Exendin PET prior to surgery. The images were evaluated in three settings a) standard clinical reading b) blinded expert reading and c) joined reading. Target (lesion) / non target (normal pancreas) ratio were determined using maximum standard uptake value (SUV_{max}). Image quality was rated by pediatric surgeons in a questionnaire.

Results

Fourteen/nineteen patients having focal lesions underwent surgery. Based on clinical readings, the sensitivity of Exendin PET (100% (confidence interval 77-100%)) was higher than that of DOPA PET (71% (confidence interval 42-92%)). Interobserver agreement between readings was higher for Exendin than for DOPA PET (Fleiss' kappa 0.91 vs. 0.56). Exendin PET provided significantly ($p=0.021$) higher target / non target ratios (2.02 ± 0.65) than DOPA PET (1.40 ± 0.40). On a five point scale, Pediatric surgeons rated Exendin PET superior to DOPA PET.

Conclusion

Exendin PET has higher clinical sensitivity and better interobserver correlation for the detection of focal CHI than DOPA PET. Better contrast and image quality makes Exendin PET superior to DOPA PET in surgeons' intra-operative quest for lesion localization.

Keywords: Congenital hyperinsulinism, Focal CHI, diagnostic imaging, Exendin PET, DOPA PET,

INTRODUCTION

CHI is the most common cause of persistent and recurrent hypoglycemia in neonates. It occurs with an incidence of 1 in 35,000-40,000 births (*1*). CHI often presents in neonates with poor feeding, seizures, jitteriness, hypotonia, apnea, cyanosis, hypothermia or a hypoglycemia-induced life-threatening event (*2*). CHI can also present in infancy or childhood and in rare cases even in adolescents or young adults (*3*). To avoid brain injury, early diagnosis and proper treatment of CHI are crucial. The diagnosis of CHI is based on clinical findings and hypoglycemic events, combined with inappropriately high insulin or C-peptide levels or low insulin-like growth factor-binding protein 1 levels (*4,5*). In diffuse CHI, which accounts for 60-70% of all cases, there is diffuse involvement of the pancreatic beta cells with enlarged hyperfunctioning cells with abnormally large nuclei and abundant cytoplasm (*6,7*). This subform is caused by recessive or dominant mutations in the *ABCC8* or *KCNJ11* genes, encoding for the beta cell ATP-sensitive potassium channels. Diffuse CHI is primarily treated with medication, such as octreotide and diazoxide. However, many patients with recessive mutations in the *ABCC8* and *KCNJ11* genes are unresponsive to this therapy and near-total pancreatectomy may then be the only option to avoid devastating hypoglycemia. Even after such an invasive, procedure, some children present with recurring hypoglycemia, requiring further treatment with medication or even re-operation (*8*).

Focal CHI accounts for 30-40% of all CHI cases associated with the K_{ATP} channel genes. This form is characterized by focal adenomatous islet cell hyperplasia caused by the concurrence of a paternal mutation in the *ABCC8* or *KCNJ11* gene and somatic loss of heterozygocity of the maternal chromosome 11p15 region within a limited pancreatic region (*9,10*). Because there is only involvement of a specific pancreatic area, focal CHI can be treated successfully by partial pancreatectomy or limited lesionectomy, which can cure the disease in case of complete removal of the lesion (*7*). Since focal CHI can be treated with much less invasive surgery than diffuse CHI, correct differentiation between these subforms is of great importance. Also, precise pre-surgical localization of the focal lesion is important for correct surgical

planning and optimization of surgical outcomes. If the lesion resides in the body or tail of the pancreas, a minimally invasive, laparoscopic procedure may be performed (*11*).

The current standard imaging technique for non-invasive detection of focal CHI is ^{18}fluoro-L-dioxyphenylalanine (^{18}F-DOPA) PET/CT (DOPA PET) (*12*). This technique was shown to have a sensitivity of 85%-89% for the detection of focal CHI (*13*), so in some cases focal lesions are still missed. In this study, we use a new radiotracer based on the peptide exendin-4, which specifically binds to the GLP-1R expressed on pancreatic beta cells with high affinity (*14*). ^{68}Ga-labeled Exendin has been shown to detect insulinomas with high sensitivity (*15,16*). The specific tracer used in the current study, ^{68}Ga-NODAGA-exendin-4, is currently being assessed in a large prospective trial for insulinoma imaging (NCT03189953). We have analyzed data of patients with CHI who underwent both DOPA PET and PET/CT using ^{68}Ga-NODAGA-exendin-4 (Exendin PET) to compare the effectiveness of these two imaging techniques for the detection and localization of focal CHI.

METHODS

Study design and patients

In this prospective multicenter study (NCT03768518), consecutive eligible patients were included at the Great Ormond Street Hospital London in the United Kingdom (7 patients) and the Radboud University Medical Center Nijmegen in The Netherlands (1 patient). Patients recruitment was performed directly in these centers and by referral from several tertiary centers across Europe.

Patients were enrolled with biochemically proven, endogenous CHI who were unresponsive to medical treatment and qualified for DOPA PET based on mutation analysis (no genetically proven diffuse CHI based on a homozygous or compound heterozygous *ABCC8/KCNJ11* mutation). Exclusion criteria were renal insufficiency (creatinine clearance < 40 ml/min) and evidence of other malignancies than insulin producing lesions. The study was approved by the local institutional review board of all participating institutes. Parents of all included patients provided written informed consent in accordance with provisions of the Declaration of Helsinki.

In addition, real world evidence data from CHI patients diagnosed and treated at the Charité University Hospital Berlin in Germany (11 patients) were analyzed in accordance with national drug regulations. Parents of these patients provided written informed consent for the use of the new radiotracer.

Procedures

In all patients, DOPA PET was performed according to the local guidelines for focal CHI detection. ^{18}F-DOPA (3 MBq/kg, lower limit: 40 MBq) was injected as a slow bolus over one minute. Patients were not fasted and not pre-treated with carbidopa. A PET/CT acquisition of one bed position for ten minutes was started 20 minutes after tracer injection. Depending on assessment of the first scan, additional PET acquisitions were performed at 40 and/or 60 minutes after tracer injection.

For Exendin PET, ^{68}Ga-NODAGA-exendin-4 (1.6±0.1 MBq/kg, lower limit: 20 MBq, corresponding to a peptide dose of maximally 0.08-0.12 µg/kg, lower limit: 1.4 µg) was injected intravenously as a slow bolus over five minutes. Details on radiopharmaceutical preparation are provided as a supplement. Patients were fasted for one hour prior to tracer injection to reduce endogenous GLP-1 production. Blood glucose levels were monitored before, and at least at 5, 10, 15, 30, 60, 90 and 120 minutes after tracer injection. Since blood glucose levels may decrease after exendin injection, close monitoring was performed. Intravenous glucose injection with a case-specific infusion rate was given to all patients to manage glucose levels during the procedure.

PET acquisition methods varied because of differences in institutional standard of care for CHI patients. Details on Exendin PET and PET/MRI acquisition procedures for all centers and reconstruction parameters are given in supplemental table 1. At the Great Ormond Street Hospital London, a protocol has been developed for DOPA PET/CT to be carried out under oral sedation with chloral hydrate in children with CHI to avoid general anesthesia (manuscript in submission). This protocol was adopted for Exendin PET acquisition in London.

At the Radboudumc in Nijmegen, one patient was included. Scans in Nijmegen were performed without anesthesia with the use of a vacuum mattress.

Real world evidence from an institutional database of 11 CHI patients who underwent an Exendin PET for diagnostic purposes at the Charité University Hospital Berlin were included retrospectively. Patients were imaged under inhalation anesthesia with isoflurane under supervision of an anesthesiologist, except older children which were able to undergo the procedure without sedation.

Evaluation

Histological evaluation and clinical outcome (normalization of blood glucose levels after surgery) were used as a reference standard. Clinical reading of DOPA PET and Exendin PET scans was performed at the site of patient inclusion by non-blinded observers. The clinical reading was performed by a pediatric endocrinologist (hyperinsulinism expert) together with a nuclear medicine physician and a pediatric surgeon at the site of the PET scan. After completion of data collection, all DOPA and Exendin PET images were re-evaluated by one (MG) blinded Exendin-experienced nuclear medicine physician (expert reading). Additionally, a joint re-evaluation of all images was performed by this Exendin-experienced nuclear medicine physician together with a pediatric endocrinologist highly experienced in DOPA PET reading. All images were evaluated in terms of disease subform and, if detected, the size and location of the focal lesion. For exact localization of the focal lesion, the pancreas was divided into six areas based on anatomical relation to the pancreatic duct and portal vein (see supplemental figure 1). Images from all timepoints were used for interpretation.

Quantitative analysis of the DOPA PET and Exendin PET or PET/MR scans in which focal lesions were confirmed by histopathology, was performed by a non-blinded expert. Volumes of interest (VOIs) were drawn to determine tracer uptake expressed as SUV_{max} in different parts of the pancreas and visible focal lesions. SUV_{max} ratios of the focal lesion or area with the highest tracer uptake (in DOPA PET scans where the focal lesion was not detected) and the area with the next highest tracer uptake were determined. VOIs were drawn over the head, body and tail of the pancreas. Within these VOIs, isocontour VOIs were created consisting of the voxels with the 30% highest intensity (example of resulting VOIs are depicted in supplemental figure 2). For quantification of the dynamic PET scans, reconstructed images of the timeframe 30 to 40 minutes (Berlin) and 40 to 45 minutes (London) after injection were used.

To estimate the optimal imaging time point for Exendin PET, SUV_{max} ratios in reconstructed images of five-minute intervals over the imaging period from 0 to 45 minutes after tracer injection were determined in four patients with focal disease.

To evaluate image quality and correlation of imaging results with the intraoperative findings, DOPA PET and Exendin PET images of 13 patients with a detected focal lesion were rated by the involved pediatric surgeon using a questionnaire based on the Leiden-surgical rating scale (see supplemental material).

Statistical analysis

Imaging results confirmed by histopathology were regarded as true positives, or true negatives. Imaging results with competing histopathology results as false positives or false negatives. Ninety-five percent confidence intervals for sensitivity were calculated using the Clopper-Pearson method. Interobserver variation was calculated using Fleiss' kappa. SUV_{max} ratios in DOPA PET and Exendin PET scans were compared using paired sample T-tests. Surgeon scores of image quality were compared using Wilcoxon signed rank tests. Statistical analyses were performed using SPSS (version 22; SPSS, Chicago, IL).

RESULTS

Patients

We included data of 19 CHI patients. Baseline characteristics of the patients are given in table 1 and clinical details in supplemental table 2. All patients underwent DOPA PET and Exendin PET, with a median time of 13 (4–72) days between the procedures. Upon clinical reading, DOPA PET revealed focal areas of high tracer uptake suspicious for focal lesions in ten patients (53%) and Exendin PET in 14 patients (74%) (Table 2). The study profile is depicted in supplemental figure 3.

Tolerability

One patient (5%) experienced vomiting following injection of ^{68}Ga-exendin. In two patients (11%), episodes of mild hypoglycemia requiring increased glucose infusion occurred following injection of ^{68}Ga-

exendin,. In the other patients, glucose levels were stable (> 3.5 mmol/L) under regular monitoring and intravenous glucose infusion. No other adverse events occurred in any of the patients.

Surgery

Results of both imaging procedures were used for surgical planning. Suspicious lesions were detected by clinical reading of the PET images in 14 patients. These patients underwent surgery and presence of focal lesions was confirmed by histopathological evaluation. All surgically treated patients with focal lesions were cured after surgery (normalization of blood glucose levels in long-term follow-up).

Of the remaining five patients, in which no focal lesion was detected by clinical reading (diffuse tracer uptake on both DOPA and Exendin PET), one patient underwent near-total pancreatectomy because of insufficient response to medication. In line with the imaging results, histopathology indicated diffuse disease in this patient. The four patients that did not undergo surgery (aged 10, 18, 68 and 125 months) could be sufficiently managed with diet and medication.

Since histopathology and clinical follow-up were the reference standard, patients who did not undergo surgery were excluded from analysis.

Diagnostic performance

Imaging results are summarized in table 2. In this patient population, Exendin PET has a sensitivity of 100% (confidence interval 77-100%) for detection of focal lesions compared to a sensitivity of 71% (confidence interval 42-92%) for DOPA PET, based on clinical readings of the images. In 4 out of 15 patients (27%), focal lesions were only identified using Exendin PET. In these patients, the surgery planning was based solely on the results of the Exendin PET. DOPA PET and Exendin PET images of these four cases are shown in figure 1. Based on the clinical readings, Exendin PET performed better for detection of focal lesions.

Interobserver correlation

Upon re-evaluation of the DOPA PET images by an expert nuclear medicine physician, two additional focal lesions were identified, increasing the sensitivity to 86% (57-98%). In the expert readings of the Exendin PET images, one focal lesion was missed, decreasing the sensitivity to 93% (66-100%). By

joint reading of the images by an expert nuclear medicine physician and a pediatric endocrinologist, all focal lesions were detected on both Exendin PET and DOPA PET. While the sensitivity of both techniques reached 100%, the interobserver agreement between the readings is higher for Exendin PET than DOPA PET (Fleiss' kappa 0.91 vs. 0.56). For Exendin PET there is almost perfect agreement while for DOPA PET, the level of agreement between the readings is only moderate. The increased sensitivity of DOPA PET only upon re-evaluation of the images, together with the higher interobserver agreement in evaluation of the Exendin PET images, clearly indicates a facilitated and more reliable interpretation of the Exendin PET images, resulting in more unequivocal results.

Semiquantitative analysis

In patients with histopathologically proven focal CHI, SUV_{max} ratios of the focal lesion to the area of the pancreas with the next highest tracer uptake are significantly higher in Exendin PET than DOPA PET (2.03±0.63 and 1.03±0.35, respectively, p=0.0026) (Figure 2). These quantitative data show that Exendin PET provides better contrast to discriminate between focal and diffuse disease, and thus explains the difference in interobserver agreement levels.

Quantification of reconstructed images of five-minute intervals over the imaging period shows some variability between patients in the timepoint of the highest SUV_{max} ratio. SUV_{max} ratios over time are depicted in supplemental figure 4. For all 4 patients, the highest SUV_{max} ratio is between 30 and 45 minutes after tracer injection. This therefore seems to be the best timeframe for Exendin PET imaging.

Surgical ease

The influence of the PET image quality on the surgical ease was measured by rating of the DOPA and Exendin PET images by the involved pediatric surgeons. These were all experienced surgeons who have performed more than 10 CHI surgeries during their career and more than 5 during the last 3 years. Rating of the PET image quality by the surgeons showed significantly higher scores for Exendin PET than for DOPA PET for the decision to perform surgery (4.5 vs. 3.8 resp., p=0.025, Figure 2B) as well as correlation of the imaging results with intra-operative findings (4.4 vs. 3.7 resp., p=0.0083, Figure 2C). Out of 13 cases, surgeons reported to prefer Exendin PET imaging for future CHI patients in 9 cases, versus DOPA PET in

only 1 case and no preference in 3 cases. This implies a better image quality of Exendin PET compared to DOPA PET and a possible benefit for the surgical treatment of CHI patients.

DISCUSSION

The results of the present study indicate that Exendin PET is a promising tool for detection and localization of focal CHI, providing a high sensitivity and diagnostic accuracy. The higher interreader agreement of Exendin PET compared to DOPA PET indicates superior performance of Exendin PET in some patients by providing more unequivocal results.

Quantitative analysis of scans of patients with histopathologically confirmed focal CHI showed significantly higher SUV_{max} ratios in Exendin PET compared to DOPA PET. The higher contrast between uptake in the focal lesion and the remainder of the pancreas in the Exendin PET scans enables easier detection of focal lesions. This explains the higher sensitivity of Exendin PET based on the initial clinical reading, and the higher rate of agreement in readings of Exendin PET images between clinical and expert readers in comparison to DOPA PET images. This is of importance, especially in cases with a heterogeneous pattern of tracer uptake in the pancreas, which are usually difficult to diagnose (*13*).

The superior image quality of Exendin PET is important for both the scan reading and the surgical procedure, since successful surgery depends on precise pre-surgical detection of focal CHI and subsequently finding and completely removing the focal lesion intraoperatively. This is reflected in the rating of the images by pediatric surgeons. Exendin PET could benefit the surgical treatment of CHI patients by facilitating the decision to perform surgery as well as the intra-operative localization of the focal lesion.

In our limited population of 19 CHI patients, 4 cases of focal CHI were clinically not identified using DOPA PET. This is a high number compared to a previous large prospective study with 50 cases and retrospective reviews of 105 and 195 cases, which reported sensitivities of 88%, 85%, and 89% respectively, for detection of focal CHI using DOPA PET (*13,17,18*). This is suggestive of a high complexity of the cases in this study. An overrepresentation of such difficult cases in our study population could result from an increased incentive to refer patients with complex and equivocal DOPA PET imaging results for an

investigative diagnostic procedure. In this population, Exendin PET outperformed DOPA PET in the clinical non-expert setting, facilitating curative surgery without the need for further medicinal treatment or near-total pancreatectomy in 4 additional patients. Exendin PET therefore had a major positive impact on the clinical management of these patients.

A limitation of the current study is the inability to exclude the possibility of missed focal lesions. All focal lesions that were identified by Exendin PET were confirmed by histopathology. However, 4 patients in which both DOPA PET and Exendin PET indicated diffuse disease, did not undergo surgery, but received continued medical treatment. In these patients, diffuse disease is not confirmed.

Another possible limitation of this study is the inclusion of patients from three centers with differences in the Exendin PET acquisition procedure (see Supplemental Table 1). However, the high degree of diagnostic accuracy and interreader agreement of exendin PET in all the included patients shows the robustness of this technique in clinical practice.

Based on the data in this study, the expected optimal timeframe for Exendin PET imaging is between 30 and 45 minutes after tracer injection. Focal lesions in the tail of the pancreas, which overlap with the contour of the left kidney pose a diagnostic challenge with DOPA PET, which has been described previously (*13*). Because of the high renal accumulation of Exendin, this issue also occurs with Exendin PET. In such cases, performing additional scans at later time points could be beneficial, since uptake of Exendin in the kidneys was shown to decrease over time in adult patients (*19*).

The introduction of DOPA PET to discriminate between focal and diffuse CHI has had a major impact on the clinical approach to CHI patients by eliminating the need for more invasive diagnostic procedures like selective arterial calcium stimulation with simultaneous venous sampling or transhepatic portal venous insulin sampling, and by optimizing surgical treatment because of increased diagnostic accuracy. This study shows that Exendin PET has the potential to even further improve the treatment of patient with focal CHI by improving the diagnostic accuracy and certainty. This could enable the performance of curative surgery in more patients and benefit surgical planning by providing more precise and reliable pre-operative images.

In addition to the better image quality of Exendin PET compared to DOPA PET, another important advantage of Exendin PET is the production of ^{68}Ga with a generator system. Because of the short half-life of ^{68}Ga (68 minutes) it cannot be transported between centers. However, the production with a generator system enables on site production of the radiotracer even at PET centers without a cyclotron facility, thereby enabling broad availability of this tracer. Since ^{18}F-DOPA is often difficult to obtain, this could transform the care for focal CHI patients in such centers. In addition, the equivocal results provided by Exendin PET will also enable correct image interpretation in less experiences center. An additional important advantage of ^{68}Ga-exendin-4 is the very low PET radiation dose to the patients, which we previously calculated to be about four-fold lower for newborn patients than the radiation dose from ^{18}F-DOPA (*19*).

CONCLUSION

In this study, we provide the first clinical evidence for detection and localization of focal CHI using Exendin PET. These first results demonstrate a better image quality of Exendin PET compared to the standard DOPA PET, resulting in an excellent sensitivity and diagnostic accuracy, which changed the surgical management in four out of 19 patients. While the performance of Exendin PET needs to be further assessed in a larger patient population, we believe that Exendin PET has the potential to replace DOPA PET as the primary imaging tool for detection and localization of focal CHI in the future.

FINANCIAL DISCLOSURE

This work was supported by BetaCure (FP7/2014-2018, grant agreement 602812). PET/MR use at the Charité was supported by Deutsche Forschungsgemeinschaft (INST 335/543-1 FUGG).

DISCLAIMER

M Gotthardt declares that he is an inventor and holder of the patent “Invention affecting GLP-1 and exendin” (Philipps-Universität Marburg, June 17, 2009). All other authors declare they no competing interests.

ACKNOWLEDGEMENTS

The authors thank all patients and their parents/caretakers for their participation in the study. We thank the technical staff at the Radboudumc Nijmegen, Charité Berlin and University College London for their support with radiochemical preparations and PET investigations.

KEY POINTS

Question:

Is Exendin PET effective for preoperative detection and localization of focal CHI?

Pertinent findings:

Exendin PET has higher clinical sensitivity and better interobserver correlation for the detection of focal CHI than DOPA PET. Exendin PET provided significantly higher target / non target ratios than DOPA PET and pediatric surgeons rated Exendin PET superior to DOPA PET.

Implications for patient care:

Exendin PET has the potential to improve the treatment of patient with focal CHI by improving the diagnostic accuracy and certainty. This could enable the performance of curative surgery in more patients and benefit surgical planning by providing more precise and reliable pre-operative images

REFERENCES

1. Senniappan S, Shanti B, James C, Hussain K. Hyperinsulinaemic hypoglycaemia: genetic mechanisms, diagnosis and management. *J Inherit Metab Dis.* 2012;35:589-601.

2. Demirbilek H, Hussain K. Congenital Hyperinsulinism: Diagnosis and Treatment Update. *J Clin Res Pediatr Endocrinol.* 2017;9:69-87.

3. Gutgold A, Gross DJ, Glaser B, Szalat A. Diagnosis of ABCC8 Congenital Hyperinsulinism of Infancy in a 20-Year-Old Man Evaluated for Factitious Hypoglycemia. *J Clin Endocrinol Metab.* 2017;102:345-349.

4. Galcheva S, Al-Khawaga S, Hussain K. Diagnosis and management of hyperinsulinaemic hypoglycaemia. *Best Pract Res Clin Endocrinol Metab.* 2018;32:551-573.

5. Ferrara C, Patel P, Becker S, Stanley CA, Kelly A. Biomarkers of Insulin for the Diagnosis of Hyperinsulinemic Hypoglycemia in Infants and Children. *J Pediatr.* 2016;168:212-219.

6. Han B, Newbould M, Batra G, et al. Enhanced Islet Cell Nucleomegaly Defines Diffuse Congenital Hyperinsulinism in Infancy but Not Other Forms of the Disease. *Am J Clin Pathol.* 2016;145:757-768.

7. Lord K, Dzata E, Snider KE, Gallagher PR, De Leon DD. Clinical presentation and management of children with diffuse and focal hyperinsulinism: a review of 223 cases. *J Clin Endocrinol Metab.* 2013;98:E1786-1789.

8. Beltrand J, Caquard M, Arnoux JB, et al. Glucose metabolism in 105 children and adolescents after pancreatectomy for congenital hyperinsulinism. *Diabetes Care.* 2012;35:198-203.

9. Fournet JC, Mayaud C, de Lonlay P, et al. Unbalanced expression of 11p15 imprinted genes in focal forms of congenital hyperinsulinism: association with a reduction to homozygosity of a mutation in ABCC8 or KCNJ11. *Am J Pathol.* 2001;158:2177-2184.

10. Verkarre V, Fournet JC, de Lonlay P, et al. Paternal mutation of the sulfonylurea receptor (SUR1) gene and maternal loss of 11p15 imprinted genes lead to persistent hyperinsulinism in focal adenomatous hyperplasia. *J Clin Invest.* 1998;102:1286-1291.

11. Bax KN, van der Zee DC. The laparoscopic approach toward hyperinsulinism in children. *Semin Pediatr Surg.* 2007;16:245-251.

12. Otonkoski T, Nanto-Salonen K, Seppanen M, et al. Noninvasive diagnosis of focal hyperinsulinism of infancy with [18F]-DOPA positron emission tomography. *Diabetes.* 2006;55:13-18.

13. Laje P, States LJ, Zhuang H, et al. Accuracy of PET/CT Scan in the diagnosis of the focal form of congenital hyperinsulinism. *J Pediatr Surg.* 2013;48:388-393.

14. Brom M, Oyen WJ, Joosten L, Gotthardt M, Boerman OC. 68Ga-labelled exendin-3, a new agent for the detection of insulinomas with PET. *Eur J Nucl Med Mol Imaging.* 2010;37:1345-1355.

15. Antwi K, Fani M, Heye T, et al. Comparison of glucagon-like peptide-1 receptor (GLP-1R) PET/CT, SPECT/CT and 3T MRI for the localisation of occult insulinomas: evaluation of diagnostic accuracy in a prospective crossover imaging study. *Eur J Nucl Med Mol Imaging.* 2018;45:2318-2327.

16. Antwi K, Fani M, Nicolas G, et al. Localization of Hidden Insulinomas with (6)(8)Ga-DOTA-Exendin-4 PET/CT: A Pilot Study. *J Nucl Med.* 2015;56:1075-1078.

17. Hardy OT, Hernandez-Pampaloni M, Saffer JR, et al. Diagnosis and localization of focal congenital hyperinsulinism by 18F-fluorodopa PET scan. *J Pediatr.* 2007;150:140-145.

18. Treglia G, Mirk P, Giordano A, Rufini V. Diagnostic performance of fluorine-18-dihydroxyphenylalanine positron emission tomography in diagnosing and localizing the focal form of congenital hyperinsulinism: a meta-analysis. *Pediatr Radiol.* 2012;42:1372-1379.

19. Boss M, Buitinga M, Jansen TJP, Brom M, Visser EP, Gotthardt M. PET-Based Human Dosimetry of (68)Ga-NODAGA-Exendin-4, a Tracer for beta-Cell Imaging. *J Nucl Med.* 2020;61:112-116.

Figures

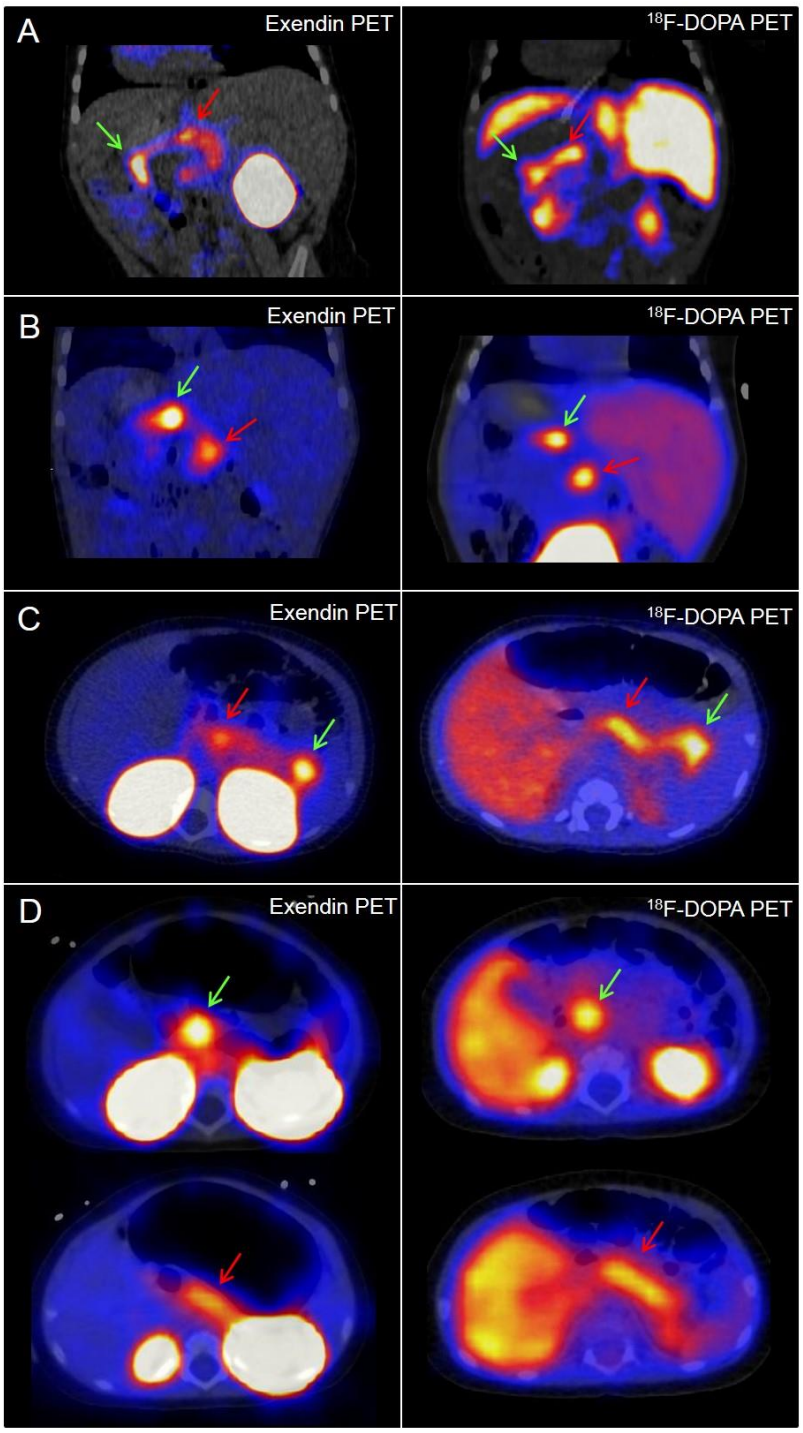

Figure 1: Exendin PET and DOPA PET images of patient 2 (A), patient 4 (B), patient 6 (C) and patient 9 (D), in which Exendin PET scans were reported as focal while DOPA PET scans were reported as diffuse in clinical readings. Locations of the focal lesions (for DOPA PET detected during joined readings) are indicated with green arrows. In D, the focal lesion in the head is indicated with green arrows and for comparison tracer uptake in the tail is indicated with red arrows. Presence of focal lesions was confirmed by histopathology in all four patients.

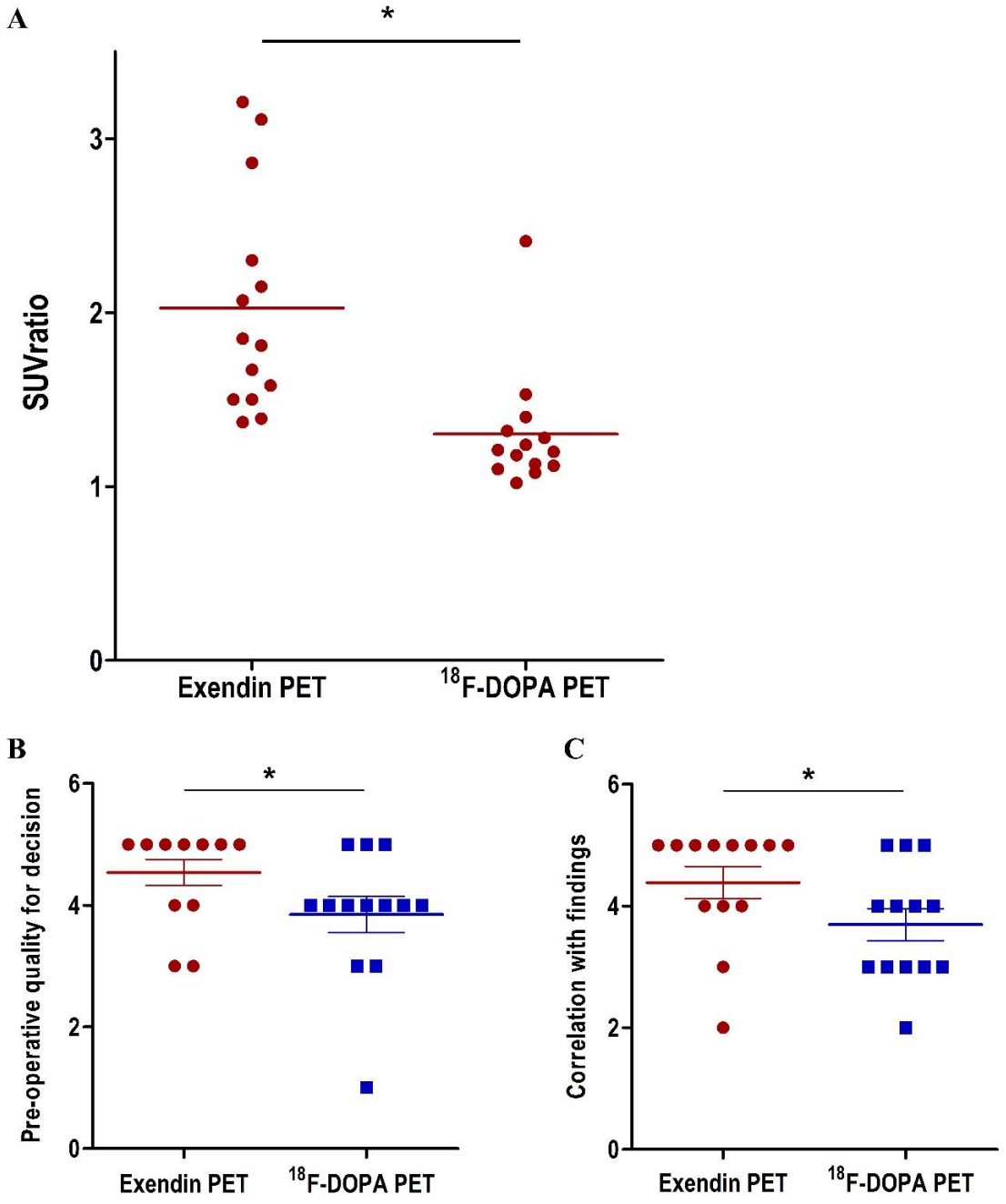

Figure 2: (A) SUV_{max} ratios between the focal lesion and the area with the next highest tracer uptake. Date are given as mean ± SD as well as individual datapoints. Scans with identified focal lesions during clinical reading are depicted in red. Scans reported to show diffuse disease are depicted in blue. (B,C) Rating scores of Exendin and DOPA PET images by pediatric surgeons. Scores on preoperative image quality for the decision to perform surgery (B) and correlation of imaging results with intraoperative findings (C). * Indicates $p<0.05$.

Tables

Participants (n=19)	
Age (months)	8.3 (4.0 – 22.0)
Age at diagnosis (days)	7 (1.5 – 12)
Sex	
Female	8/19 (42%)
Male	11/19 (58%)
Genetic mutation	
Paternal ABCC8 mutation	16/19 (84%)
No or unknown mutation	3/19 (16%)
Response to medication	
Full	5/19 (26%)
Partial	14/19 (74%)

Table 1: Patient characteristics. Data are given as median and interquartile range or number/total and percentage

	DOPA PET	Exendin PET
Focal lesions detected (clinical reading)	10/14 (71%)	14/14 (100%)
True positives (clinical reading)	10	14
False negatives (clinical reading)	4	0
Sensitivity		
Based on clinical reading	71% (42 – 92%)	100% (77 – 100%)
Based on expert reading	86% (57 – 98%)	93% (66 – 100%)
Based on joint reading	100% (77 – 100%)	100% (77 – 100%)

Table 2: Sensitivity of DOPA PET and Exendin PET based on clinical and study readings, given as value and 95% confidence interval, and percentages of agreement between readings. Sensitivity is calculated for cases with focal lesions only.

Supplemental material

Radiopharmaceutical preparation of ^{68}Ga-NODAGA-exendin-4

Exendin-NODAGA peptide was purchased from PiChem (Graz, Austria) as freeze-dried aliquots. GRP synthesizer module was purchased from Scintomics GmbH, Germany and Modular Lab PharmTracer synthesis module from Eckert & Ziegler GmbH, Germany. Hydrochloric acid (HCl) was supplied by Rotem Industries Ltd. $^{68}GaCl_3$ was obtained from 1850 MBq ^{68}Ge/^{68}Ga generator (Galliapharm®, Eckert & Ziegler GmbH, Germany), SEPPAK C8 Plus Light Cartridges (C8) were purchased from Waters, UK and Chromafix® PS-H+ (small) from Macherey Nagel™, Germany. All other components were acquired as one disposable kit (Reagent and hardware kit for synthesis of ^{68}Ga peptides using cationic purification) from ABX GmbH, Germany.

GRP Synthesizer Module (RadboudUMC Nijmegen)

The generator was eluted with 10 ml of 0.1 N HCl and ^{68}Ga was trapped on a polystyrene-H^+ (PS-H^+) cartridge. The cartridge was then eluted with 1.5 ml of 5M NaCl in 0.1 M HCl (eluent) into the reaction vial, containing 200 µl of exendin-NODAGA (10 µg of peptide in water for injection (WFI)), 475 µl of 2.5 M 4-(2-hydroxyethyl)-1-piperazineethanesulfonic acid (HEPES) buffer and 50 µl ascorbic acid (100 mg/ml in WFI). After 15 minutes incubation at 100°C, the vessel is cooled and 2 ml ethylenediaminetetraacetic acid (EDTA), 50 mM/polysorbate 80 0.15% is added. ^{68}Ga-NODAGA-exendin-4 was purified on a HLB cartridge, sterilized by passing through a 0.2 µm filter (millex GV) and diluted with saline.

Modular Lab PharmTracer Module (Charité Berlin and UCLH London)

The C18 cartridge of the cassette (C4-GA68-AFPP) was replaced by a C8 cartridge and the STRATA X cartridge was replaced by a PS-H^+ cartridge (s) after pre-conditioning with 2ml of eluent followed by 5 ml of WFI. The generator was then eluted with 10 ml of 0.1 N HCl and ^{68}Ga was trapped on the PS-H^+(s) cartridge. The cartridge was eluted with 1.7 ml of eluent into the reaction vial, containing 200 µl exendin-NODAGA (10 µg of peptide in WFI), 475 µl of 2.5 M HEPES buffer and 50 µl ascorbic acid (100 mg/ml in WFI). After 10 minutes incubation at 85 °C, the reactor was allowed to cool down to 70° C before adding 2 ml of EDTA, 50 mM/polysorbate 80 0.15%. ^{68}Ga-NODAGA-exendin-4 was purified on a C8 cartridge, sterilized by passing through a 0.2 µm filter (millex GV) and diluted with saline.

Quality controls were performed on Radio-HPLC and Radio-TLC systems with a radiochemical purity of ≥ 95%. The pH of the tracer was around 6, the radiochemical yield and the molar specific activity were determined to be 50-60% and 175-200 MBq/nmol, respectively.

Surgeon questionnaire

The questionnaire for the pediatric surgeons, used to assess image quality and correlation of imaging results with intra-operative findings, contained the following questions:

1) How many CHI surgeries have you performed during your career?

1. > 10
2. < 10

2) How many CHI surgeries have you performed during the last 3 years

1. > 5
2. < 5

3) How do you rate the preoperative image quality for your decision on performing surgery? lesion? Please rate according to the following scale:

1. Image quality extremely poor for decision making
2. Image quality poor for decision making
3. Image quality acceptable for decision making
4. Image quality good for decision making
5. Image quality optimal for decision making

4) How well did the imaging results correlate with the intraoperative findings? Please rate according to the following scale:

1. Extremely poor correlation with intra-operative findings
2. Poor correlation with intra-operative findings
3. Acceptable correlation with intra-operative findings
4. Good correlation with intra-operative findings
5. Optimal correlation with intra-operative findings

5) Which imaging modality would you prefer for future CHI patients?

UCLH London	
Scanner	PET/CT: Discovery PET/CT 710 scanner (GE Healthcare)
PET acquisition	List mode, start with tracer injection, 50 min duration
PET reconstruction	2 iterations, 24 subsets, standard Z filter 5 mm, 256x256 matrix
CT parameters	Low-dose CT scan without contrast, 100 kV, modulated between 10 and 210 mA, slice thickness 5 mm, 50 cm field of view
RadboudUMC Nijmegen	
Scanner	PET/CT: Biograph mCT-40 time-of-flight (Siemens)
PET acquisition	Static, started 45 minutes after tracer injection, 10 min duration
PET reconstruction	3 iterations, 21 subsets, post-reconstruction Gaussian filter of 3 mm in full width at half maximum, 200x200 matrix
CT parameters	Low-dose CT scan without contrast, 120 kV, 50mA, slice thickness 5 mm, 780 mm field of view
Charité Berlin	
Scanner	PET/CT: Philips Gemini TF16 ASTONISH PET/MRI: Siemens Biograph mMR
PET acquisition	PET/CT: dynamic, started with tracer injection, 40 min duration PET/MRI: List mode, started with tracer injection, 1 hour duration
PET reconstruction	PET/CT + PET/MRI: 8 frames à 5 min; 20 min p.i. 1 frame à 10 min; 30 min p.i. 1 frame à 10 min PET/CT: BLOB-OS-TF, reconstruction filter "smooth", 144x144, 4.0x4.0x4.0 mm PET/MR: 3 iterations, 21 subsets, post-reconstruction Gaussian filter of 4 mm, 172x172 matrix, pixel spacing 4.2x4.2x2.0 mm
CT parameters	Low-dose CT without contrast, 100 kV, modulated between 10 and 210 mA, slice thickness 5 mm, 50 cm field of view
MRI parameters	Attenuation: STARVIBE, TR 3.9 ms, TE 1.2 ms, Alpha 10.6° Additional sequences: axial HASTE, axial STARVIBE, coronal T2-STIR / TIRM

Supplemental table 1: Imaging and reconstruction parameters of Exendin PET.

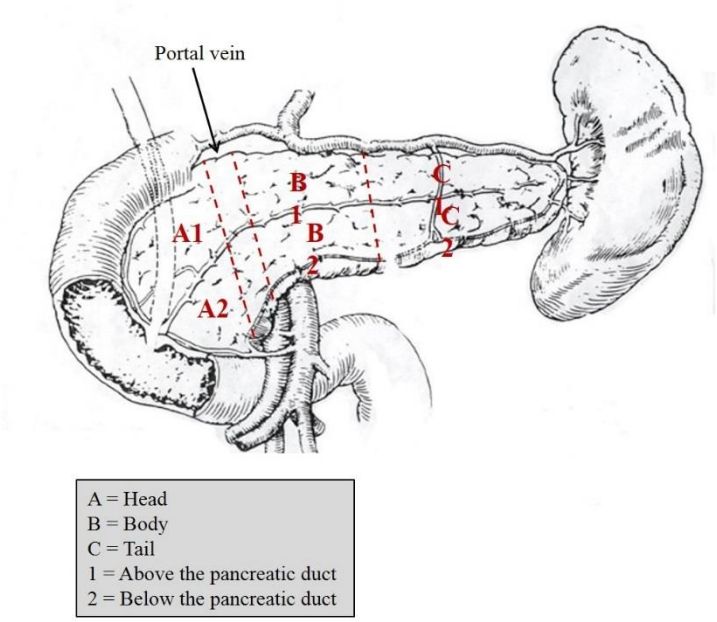

Supplemental figure 1: Image used for annotation of location of focus within the pancreas

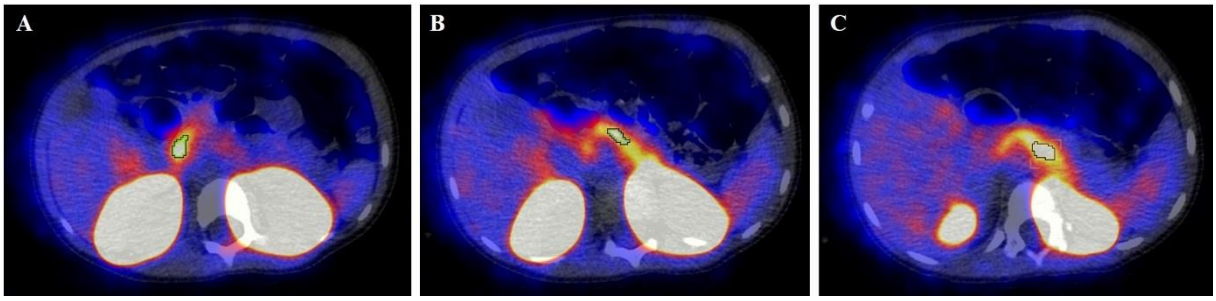

Supplemental figure 2: ROIs created of the voxels with the 30% highest intensity in the head (A), body (B) and tail (C) of the pancreas, used to calculate SUV_{max} ratios.

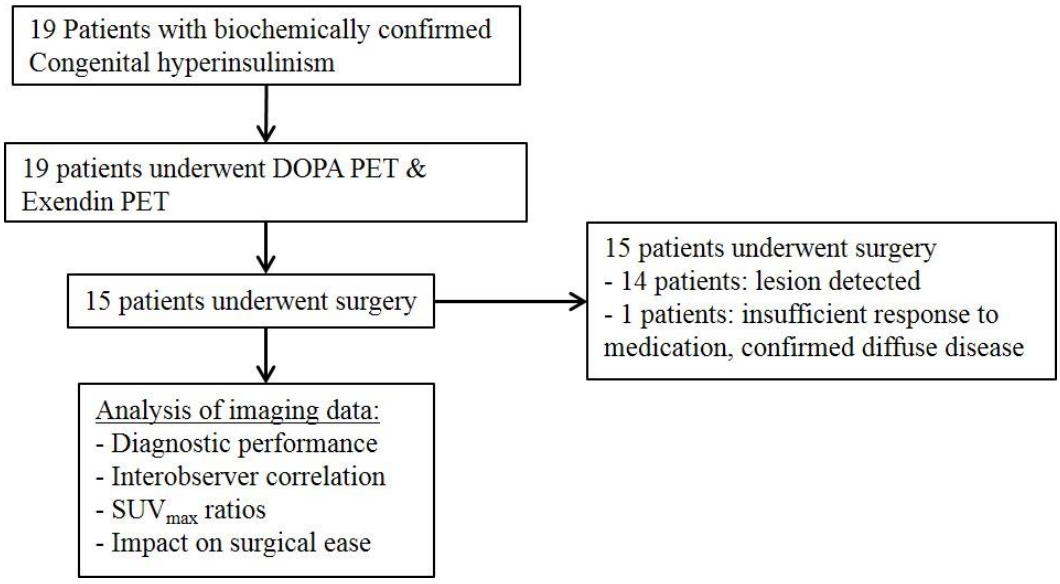

Supplemental figure 3: study profile

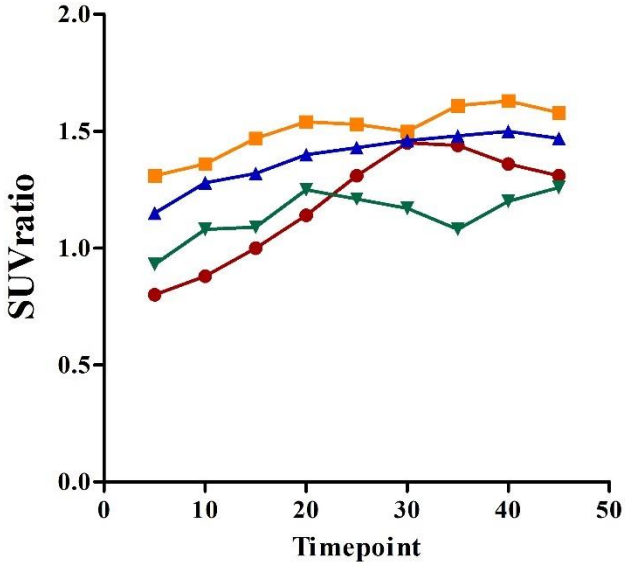

Supplemental Figure 4: SUV_{max} ratios in Exendin PET images at different imaging timepoints of 4 patients with detected focal lesions.

Patient nr	Age (months)	Results of mutation analysis	Treatment	Treatment response	Clinical reading Dopa PET	Clinical reading Exendin PET	Type of surgery	Histopathology
1	18	Paternally inherited ABCC8 mutation	Lanreotide + gastrostomy feeds	Partial	Diffuse	Diffuse	No surgery	NA
2	22	Paternally inherited ABCC8 mutation	Octreotide + Diazoxide + gastrostomy feeds	Partial	Diffuse	Focal	Enucleation	Focal
3	125	Paternally inherited ABCC8 mutation	Octreotide, switched to Lanreotide	Full response to Lanreotide	Diffuse	Diffuse	No surgery	NA
4	50	Paternally inherited ABCC8 mutation	Octreotide + gastrostomy feeds	Partial	Diffuse	Focal	Enucleation	Focal
5	61	Paternally inherited ABCC8 mutation	Octreotide + Sirolimus + gastrostomy feeds	Partial	Focal	Focal	Enucleation	Focal
6	12	Paternally inherited ABCC8 mutation	Octreotide	Full	Diffuse	Focal	Enucleation	Focal
7	8	Paternally inherited ABCC8 mutation	Octreotide + gastrostomy feeds	Partial	Focal	Focal	Enucleation	Focal
8	8	Paternally inherited ABCC8 mutation	Octreotide	Partial	Focal	Focal	Partial pancreatectomy	Focal
9	4	Paternally inherited ABCC8 mutation	Octreotide	Full	Diffuse	Focal	Partial pancreatectomy	Focal
10	5	Paternally inherited ABCC8 mutation	Octreotide + Diazoxide	Partial (limited)	Diffuse	Diffuse	(near) total pancreatectomy	Diffuse
11	2	Paternally inherited ABCC8 mutation	Octreotide	Partial	Focal	Focal	Partial pancreatectomy	Focal
12	2	Paternally inherited ABCC8 mutation	Octreotide (continuous)	Partial	Focal	Focal	Enucleation	Focal
13	9	Paternally inherited ABCC8 mutation	Octreotide	Partial	Focal	Focal	Partial pancreatectomy	Focal
14	10	Unknown (no mutation in ATP-sensitive potassium channel)	Octreotide + Diazoxide + gastrostomy feeds	Partial	Diffuse	Diffuse	No surgery	NA
15	68	No mutation in known CHI-genes	Diazoxide	Partial/full	Diffuse	Diffuse	No surgery	NA
16	4	No mutation in known CHI-genes	Octreotide	Full	Focal	Focal	Enucleation	Focal
17	4	Paternally inherited ABCC8 mutation	Octreotide	Partial	Focal	Focal	Partial pancreatectomy	Focal
18	6	Paternally inherited ABCC8 mutation	Octreotide	Full	Focal	Focal	Partial pancreatectomy	Focal
19	3	Paternally inherited ABCC8 mutation	Octreotide	Partial	Focal	Focal	Partial pancreatectomy	Focal

Supplemental table 2: Pre-operative clinical patient data